UNIVERSITY OF
ROCHESTER

DEPARTMENT OF CHEMISTRY
CHM 252 W. Udo Schröder

Molecular Collisions

Of particular interest for chemistry and physics are collisions between gas particles, i.e., ***interactions between particles***, neglected in the most elementary kinetic theory of gases. As explained previously, one is in serious difficulty to explain the premises of the ideal-gas model, with its random motion of the gas particles and their characteristic velocity distribution, without invoking, at least implicitly, interactions between the gas particles. ***For a rigorously ideal gas (colliding at most with perfectly reflective rigid walls), the speeds (magnitude of velocity) of all particles remain forever unchanged***. The motion of such ideal-gas particles is strictly along straight lines. There is no obvious reason for random motion, except for particular, e.g., stadium-like wall geometries. ***Without interactions, a multi-particle system, more generally a system with many degrees of freedom, will not evolve towards its eventual steady state (equilibrium)***, unless it already is in that state. All so-called ***transport processes***, such as diffusion, dissipation, friction, etc., are dependent on the existence of particle-particle interactions. In the following, a few examples of a simple type of interaction are considered: elastic scattering of atoms at a central potential representing the interaction between any two identical atoms.

The **Lennard-Jones potential** is a suitable candidate to model such interactions, as has been demonstrated earlier. For simplicity, one can consider the scattering in the ***rest frame*** of the "***target***" atom hit by a "***projectile***". The ***non-centrality*** (off-center) of the collision is indicated by the collision ***impact parameter b***, defined as the distance between two

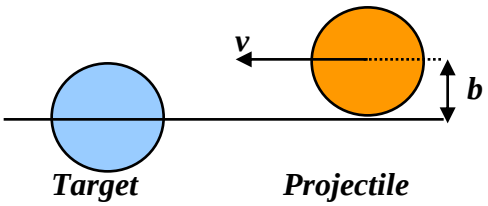

Figure 1

parallels through the centers of projectile and target, aligned with the direction of motion of the projectile (see sketch above). Such collisions for *Ar* atoms can be explored with the *MATHCAD* code MATHCAD_252\Potential_Scatter.mcd. The figures (Fig. 2) below show collision trajectories for a projectile with a velocity (v_{rel} =-*0.2 nm/ps*) typical for a temperature of *T = 60K*. The position of the fixed target (and that of the center of the potential) is indicated by a blue circle at the origin of the coordinate system. The projectile starts out at the upper right (at *1 nm* horizontal distance), with its initial velocity parallel to the abscissa. The impact parameter is large

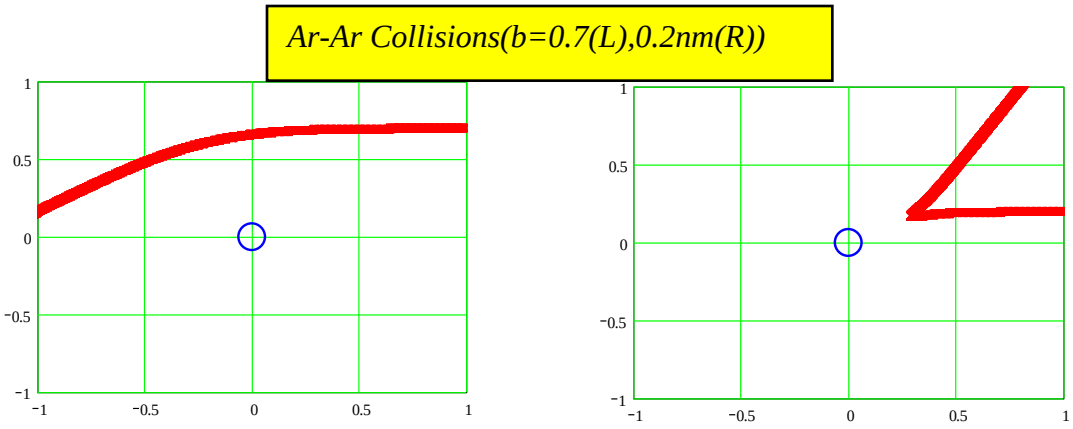

Figure 2: Peripheral (left) and central (right) collision

for the trajectory on the left (*b=0.7nm*) and relatively small for the trajectory pictured on the right (*b=0.2nm*).

Animations of these collisions can also be activated, for the series of decreasing impact parameters of *b=0.7nm*, *b=0.5nm*, *b=0.3nm*, and *b=0.1nm*. The collisions become more and more central with decreasing impact parameter, leading to trajectories of very different character. For large impact parameters *b*, there is generally only a small deflection of the path of the projectile towards the center of the potential, since the potential is attractive for large distances. The

scattering of the projectile occurs to "forward" angles, in the general direction of its original path. Because of this "grazing" character of the collision, the momentum transfer to the target atom, not considered here explicitly, is relatively small for large impact parameters.

For smaller impact parameters, however, the projectile penetrates into the inner region of the interaction potential. Since here, the repulsive core of the potential becomes dominant, the projectile is reflected back and moves quickly out of this region. Here, the change in direction of the projectile is very large, since it essentially reverses its motion. Because the collision is nearly "head-on", the momentum transfer from the projectile to the target is large. The projectile loses much, if not all, of its kinetic energy to the target.

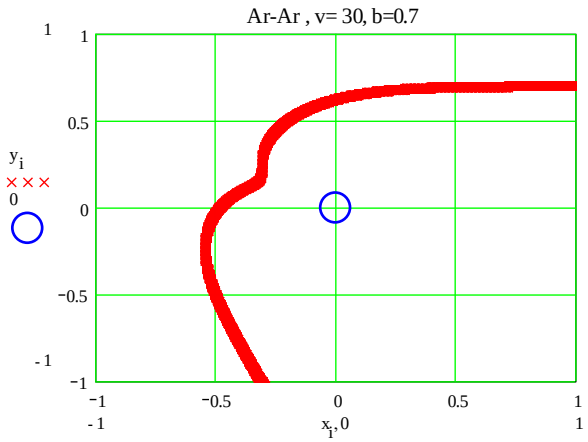

Figure 3

At lower projectile energies, the influence of the potential on the trajectory and, hence, the dependence of the scattering angle on the impact parameter, are very different from those at higher energies. This is demonstrated for the same *Ar-Ar* system and a lower relative velocity of $v_{rel} = -0.16\ nm/ps$ by the Fig. 3 on the left. Collisions may also be viewed in animated fashion for the two impact parameters of b=0.7nm and b=0.5nm.

At the higher velocity considered earlier, large impact parameters, associated with peripheral (grazing) collisions, led to forward-angle scattering. At the present, lower velocity, however, the trajectory is affected more strongly by the attractive part of the potential.

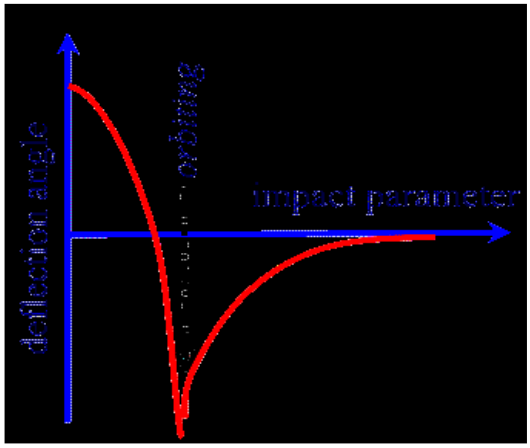

Figure 4:

Deflection function

The projectile is attracted to smaller distances, is accelerated and pulled around by the target until it hits the repulsive core of the Lennard-Jones potential. Then, it is deflected outwards again. Because its direction of motion is changed considerably in the scattering process, the momentum transfer from projectile to target can be relatively significant even at large impact parameters.

For much higher energies, the ***effect of the attractive part*** of the interaction is smaller, it is too weak to deflect the projectile much from its original path. Then, one has a simpler situation which may be described in some reasonable approximation as scattering off the hard, repulsive core of the potential, as "***hard-sphere scattering***". As will be shown below, in this limit, the scattering can be treated analytically.

The relation between scattering angle θ, the asymptotic deflection of the projectile out of its original path, and the impact parameter ***b***, is called the "***deflection function***" $\theta(b)$. This function is characteristic for the interaction between the particles, here described in terms of a conservative potential $V(r)$, the Lennard-Jones potential modeling the van der Waals interaction. As can be explored with (MATHCAD_252\Potential_Scatter.mcd), the deflection function for such a potential has two smooth, monotonic branches, indicating deterministic, orderly behavior of the scattering process. The branch at large impact parameters is characteristic for an attractive interaction, the one at smaller impact parameters is due to the repulsive core of the potential. Both branches are connected by a smooth

transition at high enough energies. At a particular (low) energy, a so-called "orbiting" singularity may develop, where the projectile orbits the target forever on a Kepler trajectory.

Sensitivity to initial Conditions in Molecular Scattering

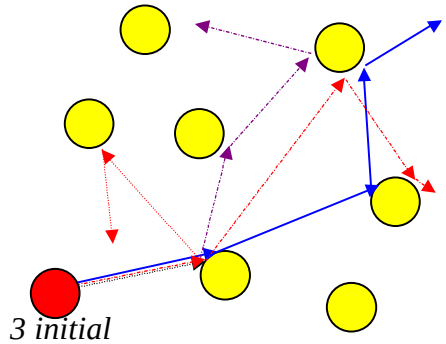

3 initial trajectories

Figure 5

In contrast to the orderly behavior of a single scattering process, the overall result of multiple scattering processes occurring in a gas of many particles is a randomization of the directions of motion of the individual particles and the smearing out of the velocity distribution. This is due to the sensitivity of the scattering angle and the transferred momentum and kinetic-energy loss on the exact conditions under which two particles collide. This sensitivity to initial conditions, can be demonstrated experimentally with MATHCAD_252\Multpl_Scatter.mcd, a simple *MATHCAD* simulation of a multiple scattering of an Ar projectile off an ensemble of Ar atoms (simulation). To prove the point under stringent conditions, multiple scattering is considered for a projectile impinging on an ordered lattice of only 12 atoms (circles), rather than a disordered gas of a much larger number of particles. The lattice constant is about 4.5 times the range of the Lennard-Jones potential used in these calculations.

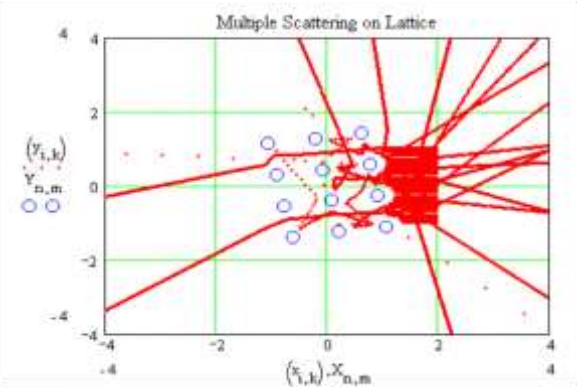

Figure 6a

Figures 6a and b illustrate the fate of 21 scattering processes with the similar initial conditions $-1nm \le y_0 = b \le +1nm$ and $x_0 = 2\ nm$. The Ar projectiles are assumed to have all the same initial velocity of $v_x = 0.58\ nm/ps$ in horizontal (x) direction. One observes clearly on the top panel of the figure, how the trajectories, all starting at $x_0 = 2\ nm$, quickly diverge after the first or second scattering. The deflection function displayed in Fig. 6b shows an erratic, non-smooth behavior. The deflection angle depends in a non-predictable fashion on the impact parameter, illustrating a high sensitivity to initial conditions.

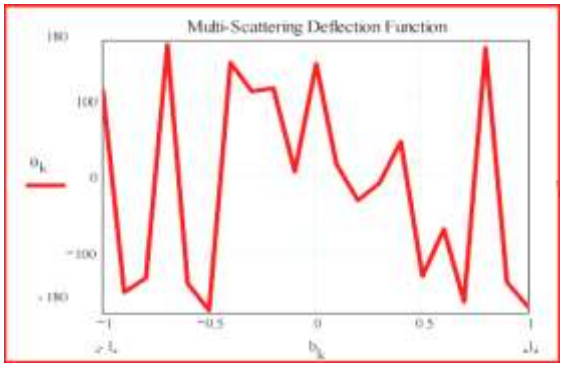

Figure 6b

This multi-scattering process must lead ***eventually (but not instantaneously!)*** to "***molecular chaos***", completely random motion of the projectiles. This is true even for scattering off an ordered lattice-like ensemble of target atoms. If the latter atoms are not bound, but freely moveable, the recoil imparted on them in the individual scattering processes will also randomize their positions and velocities. This is the basis of the random-velocity assumption made in the kinetic theory of gases.

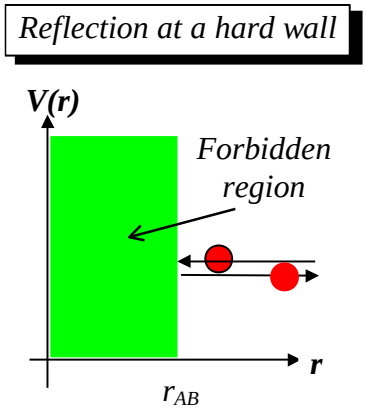

Figure 7

To simplify considerations of particle interactions, the gas particles will again be assumed to be ***structureless and to undergo purely elastic collisions***. However, they will no longer be idealized as point-like objects, but assumed to be ***rigid (hard) spheres of diameter d_i or radius R_i.*** This interaction $V(r)$ is

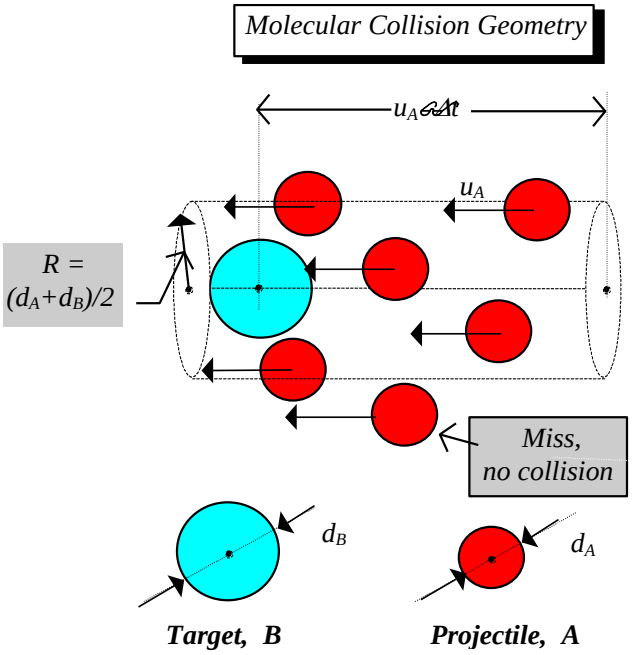

Figure 8

infinitely repulsive for center-to-center distances r between two particles A and B of less or equal to the touching distance $r_{AB} = R_A + R_B$. It is illustrated in the figure on the left showing a collision of a particle with the hard core of the potential represented by an impenetrable wall.

The geometry of collisions of ***projectile*** particles A of ***average velocity*** u_A (omit for convenience the usual bar indicating the average) with a ***target*** particle B is illustrated in the sketch. Within the time interval Δt, a number

$$\Delta N_A = \rho_A \cdot \Delta V = \rho_A \cdot \pi d_{AB}^2 \cdot u_A \cdot \Delta t = j_A \cdot \pi d_{AB}^2 \cdot \Delta t \qquad \text{(III.85)}$$

of projectiles A collide with a single given fixed target particle B,

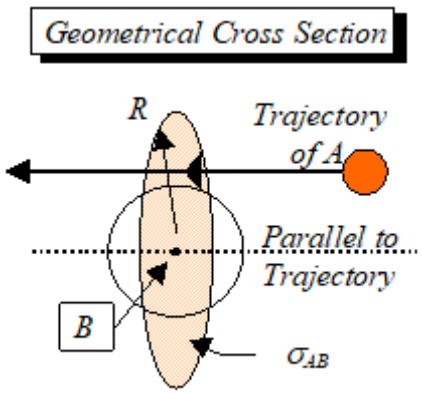

Figure 9

where $j_A = \rho_A \cdot u_A$ is the ***current density*** of the number of projectiles impinging per unit time on a unit area.

For a collision to occur, the ***distance of closest approach*** between projectile and target ***has to be smaller than the sum of the radii of target and projectile***,

$$R = d_{AB} = (1/2)(d_A + d_B) \qquad \text{(III.86)}$$

This implies that, whenever the trajectory of the projectile intercepts a disc of area

$$\sigma_{AB} = \pi R^2 \qquad \text{(III.87)}$$

drawn about the center of particle *B*, it will undergo a collision.

The expression in Equ. III.87 is termed ***geometrical cross section for a collision $A \rightarrow B$***. It can be thought of as the ***effective size of the system of the two colliding particles A and B***. More generally, the collision cross section can be imagined to be equal to the effective size of the projectile-target system, as given by the range of the interaction potential.

Equ. III.85 yields for the collision rate per target particle:

$$\frac{\Delta N_A}{\Delta t} = \rho_A u_A \sigma_{AB} = j_A \cdot \sigma_{AB} \qquad \text{(III.88)}$$

and, summed over all N_B target particles *B*, N_B times this rate. The quantity $j_A = \rho_A u_A$ is the ***current density of particles*** *A*, the ***number of particles impinging on a unit area per unit time***. With a density of particles *B* of $\rho_B = N_B/V$, one derives for the ***A-B collision rate per unit time Δt and volume V***

$$Z_{AB} = \frac{\Delta N_{AB}}{V \cdot \Delta t} = \frac{N_B}{V}\frac{\Delta N_A}{\Delta t} = \rho_A \rho_B u_{AB} \cdot \sigma_{AB} \qquad \text{(III.89)}$$

or

$$Z_{AB} = j_A \rho_B \cdot \sigma_{AB} \qquad \text{(III.90)}$$

According to Equ. III.89, the ***collision rate is proportional to the product of the densities*** ρ_A ***and*** ρ_B of the two types of particles. This is plausible, since the probability P_{AB} for two particles to meet is given by the simultaneous probability to have both particles at the same position at the same time, which is equal to the product of the probabilities $P_A \sim \rho_A$ and $P_B \sim \rho_B$ to find any of the two particles at that position. Similarly, the rate of collisions between three different particles is proportional to the product of the individual probabilities, $P_{ABC} = P_A \cdot P_B \cdot P_C$, and hence to the product $P_{ABC} \sim \rho_A \rho_B \rho_C$ of all three particle densities.

In Equ. III.89, the average velocity of projectile, as seen from a stationary target has been replaced by the ***relative velocity between target and projectile***,

$$u_{AB} = \overline{u_{AB}} = \left(\overline{u_A^2 + u_B^2}\right)^{1/2} \qquad \text{(III.91)}$$

which is the only velocity of physical interest and ***independent of the frame of reference*** chosen. The relations in Equ. III.91 will be discussed more later on.

The above formalism can be extended to the simple but interesting case of only one gas component ***A=B***. The considerations need to be modified slightly, however. In a given ***collision between two like particles***, A_1 and A_2, either A_1 can be viewed as the target (formerly ***B***), while A_2 is the projectile (formerly ***A***), ***or*** *vice versa*. Hence, every collision appears twice in a summation over the target particles if no restriction is imposed on this summation. Dividing the rate calculated with Equ. III.89 by a factor of ***2*** will account for this effect and correct for the double-counting, such that

$$Z_{AA} = \frac{\Delta N_{AA}}{V \cdot \Delta t} = \frac{1}{2}\rho_A^2 u_{AA} \cdot \sigma_{AA} = \frac{1}{2} j_A \rho_A \cdot \sigma_{AA} \qquad \text{(III.92)}$$

The difference in the procedures to calculate the number of possible collisions for gases of equal or different types of projectile and target particles is illustrated in the sketch for a simple example of *3* particles:

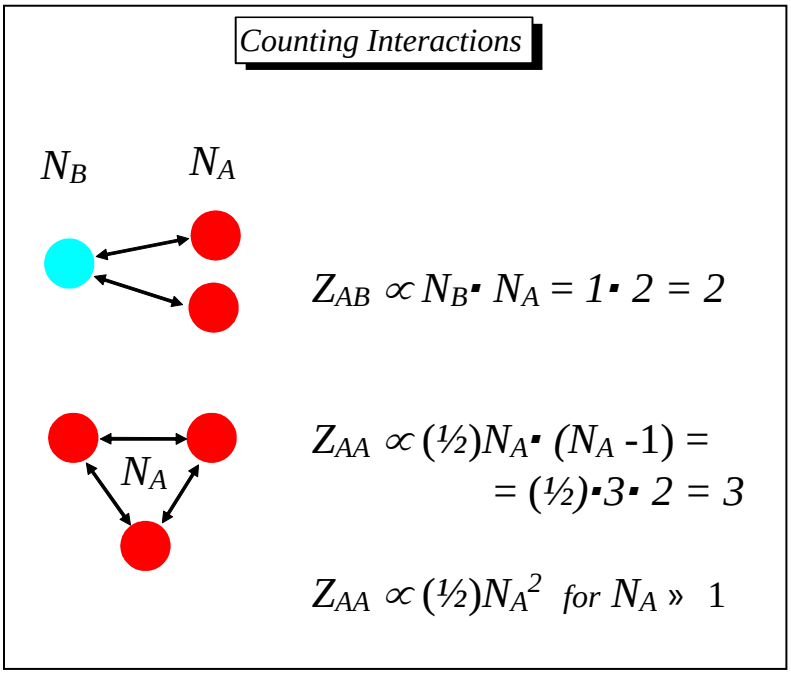

Figure 10

In the case of unequal target (***B***) and projectile (***A***) particles, the number of collisions is trivially given by the product of the numbers of targets and projectiles. However, if all particles are equal (***A***), then one can take any one of them and consider it a target, which can be hit by (N_A - *1*) projectiles. Since one has N_A such choices, the number of collisions is proportional to the product $N_A \cdot (N_A - 1)$. But, in this method of counting, any given encounter of particles ***i*** and ***j*** occurs twice, once where particle ***i*** represents the projectile and once where it stands for the target. However, the distinction between projectile and target is artificial. All that matters is the encounter, i.e., the interaction. Hence, the number of distinct interactions, represented by double arrows in the sketch, is proportional to $½N_A \cdot (N_A - 1)$. For

large numbers of particles, $(N_A\text{-}1) \approx N_A$. This then results in Equ. III.92 for the number of like-particle collisions.

Mathematically, the calculation of all possible two-body interactions between N particles is equivalent to calculating the ***number of different pairs*** that can be formed of N particles. This is given by the ***binomial coefficient***

$$\binom{N}{2} = \frac{N!}{2!\cdot(N-2)!} = \frac{1}{2}\cdot N\cdot(N-1)$$

where the ***factorial of N*** is defined as N! = $1\cdot2\cdot3\cdots N$

The relative *A*-*A* velocity varies from zero to the sum of the ***speeds*** of the two collision partners. If the velocity vectors of these two particles are independent of each other and randomly oriented, then, according to probability theory, the ***mean square speed*** is given by the sum of the squares of the individual speeds. The average of the relative speeds u_{AA} ***of the two particles*** can then be identified with the ***root-mean square speed***, ©u_A™$_{rms}$, of particle ***A***:

$$\overline{u_{AA}^2} = \overline{u_A^2 + u_A^2} = 2\overline{u_A^2} \qquad \text{(III.93a)}$$

or, defining the relative speed u_{AA} as

$$u_{AA} := \langle u_{AA} \rangle_{rms} = \sqrt{\overline{u_{AA}^2}} = \sqrt{2}\sqrt{\overline{u_A^2}} = \sqrt{2}\langle u_A \rangle_{rms} \qquad \text{(III.93b)}$$

With this average speed u_{AA}, one obtains a collision rate of

$$Z_{AA} = \Delta N_{AA} / V \exists \Delta t = (1/\sqrt{2})(\rho_A^2 \copyright u_A \text{™}_{rms}) \exists \sigma_{AA} \quad \text{(III.94)}$$

slightly different from that in Equ. III.92, because of the different definitions of the velocities u_{AA} and $\copyright u_A \text{™}_{rms}$. The collision cross section is again given by

$$\sigma_{AA} = \pi d_A^2 \quad \text{(III.95)}$$

With molecules of diameters of the order of a few times 10^{-10} m (Å) and, therefore, the corresponding cross sections of $[\sigma] \iota 10^{-19}$ m^2, particle velocities of $u_A \iota 600$ m/s, typical collision rates are of the order of a few times 10^{34} s^{-1}m^{-3}.

An important quantity characterizing a substance is the ***mean free path λ for collisions of its constituents*** and its relation to the typical dimensions of the system under consideration, e.g., the dimension of its volume. The mean free path can be calculated from the distance Δx traveled on average by a given gas particle per unit time Δt, divided by the number, ΔN_A of collisions suffered during this time. Since one is following here the path of a single chosen (projectile) particle, one has to rewrite Equ. III.88 for collisions of one projectile particle A with other, target particles, which are also of type A. In the expression for ΔN_A (Equ. III.89), the projectile speed u_A in the lab should be replaced by the average relative speed in a collision, $\boldsymbol{u_{AA} = \bigcirc\!\!\!\!2 \copyright u_A \text{™}_{rms}}$ (Equ. III.95). Since the distance traveled by the projectile is given approximately by $\boldsymbol{\Delta x = \copyright u_A \text{™}_{rms} \exists \Delta t}$, one derives

$$\lambda = \frac{u_{AA}}{\Delta N_A / \Delta t} = \frac{1}{\sqrt{2}\rho_A \cdot \sigma_{AA}} \qquad \text{(III.96)}$$

The particular definition of the relative velocity does not play a major role, since *approximately* the same velocity appears in numerator and denominator of Equ. III.96. For order-of-magnitude estimates, one can drop the square-root factor in Equ. III.96. One *should* drop this factor, if one considers the interactions of a projectile entering the gas volume with a well-defined velocity $\vec{u}$. Here, the randomized velocities of the gas particles almost averages out to zero with respect to the projectile. The important difference between this "almost" and "exactly" will be discussed in the context of friction.

The important result for λ is that the ***mean free path becomes shorter with increasing gas density ρ_{gas} and increasing collision (scattering) cross section σ_{coll}***, approximately according to

$$\lambda = \frac{|\vec{u}|}{\dot{N}_{coll}} \approx \frac{1}{\rho_{gas} \cdot \sigma_{coll}} \qquad \text{(III.96a)}$$

This realistic estimate of a constant mean free path of particles seems to imply that there is a constant average attenuation of an ensemble (e.g., a beam) of *N* projectiles in a volume of gas (or other) absorbing material. However, this is true only on an infinitesimally small scale. Consider, for example, *N* particles impinging from the left onto a slab of scattering (or absorbing) material of thickness *dx*. A constant mean free path means that the incoming flux *N* is

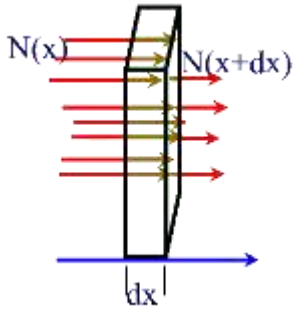

Figure 11

scattered with a probability $dP = dN/N$ that depends only on the thickness dx, and not on anything else. Then the incoming flux is reduced along the path dx

$$dN = -\alpha \cdot N \cdot dx \qquad \text{(III.97)}$$

where the quantity α is the absorption coefficient associated with this particular scattering process. Integration of Equ. III.97 leads to an exponential law for the ***flux N(x) of particles that have not been scattered*** in an absorber of thickness x:

$$N(x) = N(0) \cdot e^{-\alpha \cdot x} \qquad \text{(III.98)}$$

The transmission of the absorber, or the survival probability for the incoming particles, decreases exponentially with the absorber thickness

$$P_{surv}(x) = \frac{N(x)}{N(0)} = e^{-\alpha \cdot x} \qquad \text{(III.99)}$$

Correspondingly, the probability for collisions of projectiles with the absorber particles can be expressed as

$$P_{coll}(x) = 1 - P_{surv}(x) = \frac{N(0) - N(x)}{N(0)} = 1 - e^{-\alpha \cdot x} \qquad \text{(III.100)}$$

Hence, the absorption coefficient can easily be measured in a transmission experiment, where the number of particles penetrating and exiting the absorber is compared to the number of those impinging on it on the entrance side. The magnitude of this macroscopic

absorption coefficient α is, of course, related to the probability for the microscopic scattering process, as characterized by the scattering cross section σ_{coll}. This connection is easily established from a calculation of the mean free path, the average distance for one scattering in the absorber. Considering the case of a thin absorber, one obtains a relation between mean free path and absorption coefficient,

$$\alpha = \frac{1}{\lambda} \qquad \text{(III.101)}$$

Then, inserting expressions for α and λ, one obtains the relation

$$P_{coll}(x) = 1 - e^{-\alpha \cdot x} = 1 - e^{-x/\lambda} = 1 - e^{-\rho \cdot x \cdot \sigma_{coll}} \qquad \text{(III.102)}$$

where ρ is the density of the absorbing material (e.g., $\rho = \rho_{gas}$)

Now, the ***properties of an ideal, interaction-free gas*** ***can be specified somewhat more quantitatively*** than was possible before, when simply $p \approx 0$ was postulated: A gas can be ***considered as essentially interaction-free,*** ***an ideal gas if the mean free path is larger than the linear dimension l of the system***, i.e., $\lambda > l$, where the volume is $V \approx l^3$. Then, there is on average no interaction between a given particle and the rest of the gas, during the entire travel of the particle from one edge of the volume to the other. Nevertheless, interactions do take place and lead eventually to the equilibrium distribution of the ideal gas. The above criterion suggests that a gas may be considered as approximately ideal for pressures of the order of

$$p < \frac{k_B T}{\sigma_{coll} \cdot l} \qquad \text{(III.103)}$$

where σ_{coll} is the collision cross section.

The derivation of Equ. III.103, a ***recommended exercise***, makes use of the ideal-gas *EOS*. Hence, for a given pressure *p*, the ***gas at the higher temperature T_1 behaves more like an ideal gas than one at lower temperature $T_2 < T_1$***. This is plausible, because the pressure at higher temperature can be effected by fewer particles colliding with the container walls at higher momenta than at lower temperatures, where the number of particles in the gas and, hence, the density have to be much larger to produce the same pressure with many more individual collisions. At room temperatures, gases are close to ideal at pressures up to $10^5 Pa$ ($\leq 1\ atm$).